Available online at www.sciencedirect.com
ScienceDirect
Mathematics and Computers in Simulation 82 (2012) 1079–1092
MATHEMATICS AND COMPUTERS IN SIMULATION
www.elsevier.com/locate/matcom

Original article

Numerical implementation of the asymptotic boundary conditions for steadily propagating 2D solitons of Boussinesq type equations

Christo I. Christov *

Department of Mathematics, University of Louisiana at Lafayette, P.O. Box 1040, Lafeyette, LA 70504-1010, USA

Received 23 November 2009; received in revised form 23 July 2010; accepted 30 July 2010
Available online 10 August 2010

Abstract

In the present paper, a difference scheme on a non-uniform grid is constructed for the stationary propagating localized waves of the 2D Boussinesq equation in an infinite region. Using an argument stemming form a perturbation expansion for small wave phase speeds, the asymptotic decay of the wave profile is identified as second-order algebraic. For algebraically decaying solution a new kind of nonlocal boundary condition is derived, which allows to rigorously project the asymptotic boundary condition at the boundary of a finite-size computational box. The difference approximation of this condition together with the bifurcation condition complete the algorithm. Numerous numerical validations are performed and it is shown that the results comply with the second-order estimate for the truncation error even at the boundary lines of the grid. Results are obtained for different values of the so-called 'rotational inertia' and for different subcritical phase speeds. It is found that the limits of existence of the 2D solution roughly correspond to the similar limits on the phase speed that ensure the existence of subcritical 1D stationary propagating waves of the Boussinesq equation.

Keywords: Two-dimensional Boussinesq equation; Difference scheme; Asymptotic boundary condition; Non-uniform grid

1. Introduction

Boussinesq's equation (BE) was the first model for surface waves in shallow fluid layer that accounts for both nonlinearity and dispersion. The balance between the steepening effect of the nonlinearity and the flattening effect of the dispersion maintains the shape of the wave. The above described balance is a new paradigm in physics and can be properly termed 'Boussinesq Paradigm'. In a coordinate frame moving with the center of the propagating wave, BE reduces to Korteweg-de Vries which is widely studied in 1D.

One of the most important features of the generalized wave equations containing nonlinearity and dispersion, is that they possess solutions of type of permanent waves as shown in the original Boussinsq work [4]. In the 1960s it was discovered that these permanent waves can behave in many instances as particles (the so-called 'collision property'), and were called *solitons* by Zabusky and Kruskal [24]. Currently the coinage 'soliton' is reserved only for the particle-like waves that are solutions of a fully integrable model, such as the original Boussinesq equation. The localized waves which can retain their identity during interaction appear to be a rather pertinent model for particles, especially

* Tel.: +1 337 482 5273; fax: +1 337 482 5346.
E-mail address: christov@louisiana.edu.

0378-4754/$36.00 © 2010 IMACS. Published by Elsevier B.V. All rights reserved.
doi:10.1016/j.matcom.2010.07.030

if some mechanical properties properties (such as mass, energy, momentum) are conserved by the governing system of equations. In 1D, a plethora of deep mathematical results have been obtained for solitons [1,18]. The success was contingent upon the existence of an analytical solution of the respective nonlinear dispersive equation. As it should have been expected, most of the physical systems are not fully integrable (even in one spatial dimension) and only a numerical approach can lead to unearthing the pertinent physical mechanisms of the interactions (see, e.g., [13,15] and the literature cited therein).

The overwhelming majority of the analytical and numerical results obtained so far are for one spatial dimension, while in multidimension, much less is possible to achieve analytically, and almost nothing is known about the unsteady solutions that involve interactions, especially when full-fledged Boussinesq equations are involved. At this stage, it is of crucial importance to investigate also the 2D case, because of the different phenomenology and the practical importance. No analytical solutions are available in the literature for the Boussinesq equation. Interesting results are obtained for the so-called Kadomtsev–Petviashvili equation (KPE), which has fourth derivatives in one of the spatial direction only, while in the other direction, the highest-order derivative is second. Interesting analytical results are obtained for the solutions of KPE, which are localized in the direction with the fourth-order derivative, and are periodic in the other direction (see, e.g., [14,21,22] and the literature cited therein).

For the time being, the full Boussinesq equation still remains less amenable to analytical approaches, which requires the development of numerical techniques. Even the stationary propagating solitary waves have not been studied in detail. A preliminary numerical results were obtained in [6], but the numerical technique needed further refinement because of the difficulties in the two-dimensional case connected with the unboundedness of the region, and with the slow decay of the solution at infinity. For this reason, the first case to undergo investigation is when the wave profile is stationary in a frame moving with a prescribed phase speed. The shape of the stationary moving wave was reliably computed [8,9] using a specialized Galerkin spectral technique and shown that its decay at infinity is algebraic rather than exponential. A perturbation technique has been developed recently in [7] which confirmed the findings of [8] and put the stationary problem on more rigorous analytical footing.

In the present paper we propose a numerical algorithm which overcomes the above mentioned challenges for the numerical solution. The unboundness of the domain requires large computational box, and this is addressed by the use of non-uniform grids. Even for sufficiently large computational box, imposing a trivial Dirichlet boundary condition destroys the asymptotic behavior of the solutions as obtained numerically. To this end, a special boundary condition is derived which allows us to rigorously pose the asymptotic boundary condition at a truncated finite boundary. Here we investigate numerically the stationary propagation of localized waves for what we call Boussinesq Paradigm equation (see [11,13]). The latter involves a fourth-order spatial derivative and second-time-second-space mixed derivative.

2. Boussinesq paradigm equation (BPE)

When Boussinesq derived his famous equation [4], he demonstrated that the nonlinearity can balance dispersion and lead to the existence of waves of permanent shape that propagate in quite similar fashion as the profiles of the d'Alembert solution of the wave equation. Unfortunately, Boussinesq did some additional (and as it turns out) unnecessary assumptions, which rendered his equation incorrect in the sense of Hadamard. We term the original model the Boussinesq's Boussinesq Equation or BBE. In a nutshell, the BBE lacks the mixed fourth derivative, which together with the incorrect sign of the fourth spatial derivative was the cause of it incorrectness. It had been 'improved' in many works. The mere change of the incorrect sign of the fourth derivative in BBE yields the so-called 'good' or 'proper' Boussinesq equation, which we will refer to as the Boussinesq equation or BE. A different approach to removing the incorrectness of the BBE was discussed in [2], and the situation was remedied by changing the spatial fourth derivative a to mixed fourth derivative, which resulted into an equation is know as the Regularized Long Wave Equation (RLWE) or Benjamin–Bona–Mahony equation (BBME). In fact, the mixed derivative occurs naturally in Boussinesq derivation, and was changed by Boussinesq to a fourth spatial derivative under an assumption which is currently known a the Linear Impedance Relation (or LIA) in which is stipulated that $\partial_t \approx c\,\partial_x$. This assumption has gained quite a currency in different fields of fluid mechanics and has produced innumerable instances of unphysical results (see [16] for the case in nonlinear acoustics). An overview of the different Boussinesq equations can be found in [15], and the literature cited therein. The accurate derivation of the Boussinesq system can be found, e.g. in [13], where also the approximation is discussed that reduces the full model to a single equations termed the Boussinesq Paradigm Equation (BPE) is given. BPE equation combines both the dispersion of BBE and RLWE, and has the advantage over the more consistent model

from [13] of being a single equation. The essential mathematical difference between BBE and BPE is that the former is fully integrable (although incorrect) and the latter is not (although, it is the physically pertinent and mathematically correct model). The BPE furnishes one of those examples, which necessitates an efficient numerical treatment as a precondition for a deeper physical understanding of the problem.

The BPE is a the following two dimensional amplitude equation:

$$w_{tt} = \Delta\left[w - \alpha w^2 + \beta_1 w_{tt} - \beta_2 \Delta w\right], \tag{1}$$

where w is the surface elevation, β_1, $\beta_2 > 0$ are the two dispersion coefficients, and α is an amplitude parameter, which can be set equal to unity without loosing the generality. As already above mentioned, the main difference from BE is that for BPE one more terms is present for $\beta_1 \neq 0$ called 'rotational inertia'. A note on the notation is due here. In the original BE which is related to the water waves, the nonlinear term has a positive sign ($\alpha = 1$ in the above notations), and the soltions are actually depressions for the subcritical case. Here we have deliberately changed the sign for the sake of the presentation.

It was shown in [11,13] that the 1D PBE

$$w_{tt} = \left[w - \alpha w^2 + \beta_1 w_{tt} - \beta_2 w_{xx}\right]_{xx}, \tag{2}$$

admits a one-parameter family of soliton solutions given by

$$w^s(x,t;c) = -\frac{3}{2}\frac{c^2-1}{\alpha}\operatorname{sech}^2\left(\frac{x-ct}{2}\sqrt{\frac{c^2-1}{\beta_1 c^2 - \beta_2}}\right), \tag{3}$$

where c is the phase speed of the stationary propagating one-dimensional localized wave. Although, Eq. (2) is not fully integrable, the extensive numerical investigation from [15] based on a conservative difference scheme, succeeded to show that in its main aspects, it behaves as its fully integrable 'cousin', the BE. An important characteristic of the solitons of the 1D PBE is that they exists for $|c| > \max\{1, \sqrt{\beta_2/\beta_1}\}$ or $|c| < \min\{1, \sqrt{\beta_2/\beta_1}\}$. The first case is comprises by the so-called 'supercritical' solitons, while the latter encompasses the 'subritical' ones.

It has been recently shown in [7,8] that the 2D BPE admits stationary soliton solutions as well. Even though no analytical formula for these solutions is available, they can be accurately constructed using either a perturbation or a Galerkin spectral method. In the cited works, the way was shown of how the bifurcation nature of the problem can be addressed numerically. In the present paper we address the other main difficulty in creating difference schemes for finding the 2D Boussinesq stationary localized waves: the implementation of the asymptotic boundary conditions on a truncated domain of finite size. We set the characteristic speed of the linear waves $\gamma = 1$ and the amplitude parameter $\alpha = 1$, because it can always be eliminated by rescaling the solution. We can also select $\beta_2 = 1$. This leaves us with only one parameter, β_1, apart from the phase speed c, and we conduct a parametric study for different values of β_2 and the phase speed, c, of the stationary propagating wavers.

3. Solitary waves of BPE in the moving frame

For the numerical interaction of 2D Boussinesq solitons, one needs the shape of a stationary moving solitary wave in order to construct an initial condition. To this end, we introduce relative coordinates

$$\hat{x} = x - c_1 t, \quad \hat{y} = y - c_2 t, \tag{4}$$

in a frame moving with velocity (c_1,c_2). Since there is no evolution in the moving frame $v(x, y, t) = u(\hat{x}, \hat{y})$, and the following equation holds for u:

$$\begin{aligned}(c_1^2 u_{\hat{x}\hat{x}} + 2c_1c_2u_{\hat{x}\hat{y}} + c_2^2 u_{\hat{y}\hat{y}}) &= (u_{\hat{x}\hat{x}} + u_{\hat{y}\hat{y}}) - [(u^2)_{\hat{x}\hat{x}} + (u^2)_{\hat{y}\hat{y}})] \\ &+ \beta_1[c_1^2(u_{\hat{x}\hat{x}\hat{x}\hat{x}} + u_{\hat{x}\hat{x}\hat{y}\hat{y}}) + 2c_1c_2(u_{\hat{x}\hat{x}\hat{x}\hat{y}} + u_{\hat{x}\hat{y}\hat{y}\hat{y}}) + c_2^2(u_{\hat{x}\hat{x}\hat{y}\hat{y}} + u_{\hat{y}\hat{y}\hat{y}\hat{y}})] - \beta_2(u_{\hat{x}\hat{x}\hat{x}\hat{x}} + 2u_{\hat{x}\hat{x}\hat{y}\hat{y}} + u_{\hat{y}\hat{y}\hat{y}\hat{y}}).\end{aligned} \tag{5}$$

The so-called asymptotic boundary conditions (a.b.c.) read

$$u \to 0, \quad \text{for} \quad \hat{x} \to \pm\infty,\ \hat{y} \to \pm\infty. \tag{6}$$

The a.b.c.'s are invariant under rotation of the coordinate system, hence it is sufficient to consider solitary propagating along one of the coordinate axes, only. We chose this to be the y-axis, namely $c_1 = 0$, $c_2 = c \neq 0$. For the sake of convenience we introduce the following notations

$$\Delta \stackrel{def}{=} \partial_{\hat{x}\hat{x}} + \partial_{\hat{y}\hat{y}}, \quad D^2 \stackrel{def}{=} c^2 \partial_{\hat{y}\hat{y}}, \tag{7}$$

and recast Eq. (5) as the following system

$$\beta_2 \Delta u = \beta_1 D^2 u + u - u^2 - p(\hat{x}, \hat{y}), \tag{8}$$

$$\Delta p = D^2 u. \tag{9}$$

The trivial solution is always present for a.b.c.'s and must be avoided. In the present work we implement in a difference scheme, an idea used first in the context of spectral methods [12] and applied also in [8]. In the case of finite difference solution, it was implemented in [6]. We fix the value of the function in one point in order to prevent the iterative algorithm of 'slipping' into the trivial solution. For definiteness we take $u(0, 0) = \theta$ and consequently introduce $u = \theta\hat{u}$. Then

$$\beta_2 \Delta \hat{u} = \beta_1 D^2 \hat{u} + \hat{u} - \theta\hat{u}^2 - p(\hat{x}, \hat{y}), \tag{10a}$$

$$\Delta p = D^2 \hat{u}. \tag{10b}$$

In order not to get an overposed system, we consider θ as unknown, which is to be defined by Eq. (10a) taken at the origin. Thus

$$\hat{u}(0, 0) = 1, \quad \theta = \left. \frac{-\beta_2 \Delta \hat{u} + \hat{u} + \beta_1 D^2 \hat{u} - p}{\hat{u}^2} \right|_{\hat{x}=0, \hat{y}=0}. \tag{11}$$

Without fear of confusion we will 'reset' the names of the independent variables to x,y and omit in what follows the hat over the sought function u.

4. Projecting the asymptotic boundary conditions onto a finite boundary

Our earlier computations [6] clearly demonstrated that the asymptotic decay at infinity is much slower than the exponential decay pertinent to the 1D *sech* solitons, Eq. (3). Because of the uniform grids used in [6], we were unable to conduct numerical experiments on large enough computational boxes, which would have allowed the identification the exact behavior at infinity of the solution. This required an alternative approach which is free from the limitation of the difference approximation on a finite computational domain. Such an approach is based on a spectral approximation with a complete orthonormal system of functions (CON system) which decay at infinity [10]. An application of the said spectral method to 2D stationary propagating wave of Klein-Gordon equation was presented in [12]. The algorithm was extended to the case of PBE in [8] and the asymptotic decay of the profile of the 2D stationary propagating was found to be second-order algebraic, i.e., $u \sim r^{-2}$ for $r = \sqrt{x^2 + y^2} \to \infty$. This finding called for an approximate solution which can confirm it. Here, we follow [7] and find a regular perturbation expansion for small $\varepsilon = c^2$, where c is the above defined phase speed of the steady translation of the wave.

The asymptotic solution is presented in full detail in [7]. Here we present only the part of the derivation that suffice to identify the behavior at infinity. The idea is that even for moderate c, the asymptotic behavior is determined by the lower-order term in $\varepsilon = c^2$, and only the coefficient of the rational function describing the asymptotic behavior can change when acknowledging the higher-order terms. To this end, we refer to the connection between Cartesian and polar coordinates $x = r\cos(\theta)$, $y = r\sin(\theta)$, where θ is the polar angle. Then

$$\frac{\partial^2}{\partial y^2} \equiv \sin^2\theta \frac{\partial^2}{\partial r^2} + \frac{\cos^2\theta}{r^2} \frac{\partial^2}{\partial \theta^2} + \frac{\sin 2\theta}{r} \frac{\partial^2}{\partial r \partial \theta} - \frac{\sin 2\theta}{r^2} \frac{\partial}{\partial \theta} + \frac{\cos^2\theta}{r} \frac{\partial}{\partial r}. \tag{12}$$

We seek for a perturbation solution

$$u(x, y) = u_0(r) + \varepsilon u_1(x, y) + \varepsilon^2 u_2(x, y) + O(\varepsilon^3), \quad r = \sqrt{x^2 + y^2}, \tag{13}$$

and by neglecting the terms of order $O(\varepsilon^2)$, we get the following system for the first two coefficients of the asymptotic series.

$$\frac{1}{r}\frac{d}{dr}r\frac{d}{dr}\left[u_0(r)-u_0^2(r)-\frac{1}{r}\frac{d}{dr}r\frac{du_0}{dr}\right]=0, \tag{14a}$$

$$\varepsilon\left[-\frac{\partial^2}{\partial y^2}\left(u_0-\beta_1\frac{1}{r}\frac{d}{dr}r\frac{du_0}{dr}\right)+\Delta u_1-2\Delta(u_0u_1)-\Delta^2u_1\right]=0. \tag{14b}$$

One can seek for the solution in the following form

$$u_0(r)=F(r), \tag{15}$$

$$u_1(r,\theta)=G(r)+H(r)\cos(2\theta), \tag{16}$$

For the first term $u^{(0)}(r)=F(r)$ we have the following nonlinear equation

$$\frac{1}{r}\frac{d}{dr}r\frac{d}{dr}\left[F-F^2-\frac{1}{r}\frac{d}{dr}r\frac{dF}{dr}\right]=0 \quad\Rightarrow\quad F-F^2-\frac{1}{r}\frac{d}{dr}r\frac{dF}{dr}=A\ \ln r+B. \tag{17}$$

For a localized solution, we must set $A=B=0$. The obvious analogy of Eq. (17) to the equation for the famous *sech*-solution, hints that the sought solution does exist. It was found numerically in [7] and shown to decay slightly super-exponentially as $e^{-\alpha r}/\sqrt{r}$. The existence of the solution for $F(r)$ confirms that a bifurcation takes place and a nontrivial solution exists alongside with the trivial one. After similar manipulations we get for $G(r)$:

$$-G(r)+2F(r)G(r)+\frac{d^2G}{dr^2}+\frac{1}{r}\frac{dG}{dr}=-\frac{1}{2}\hat{F}(r)\overset{def}{=}\left[F(r)-\beta_1\frac{1}{r}\frac{d}{dr}r\frac{d}{dr}F\right]. \tag{18}$$

It was found in [7] that the function G decays slightly sub-exponentially as $e^{-\alpha r}\sqrt{r}$ for $r\to\infty$.

The radical difference of the behavior at infinity is difference comes from H, for which we get

$$\left(\frac{d^2}{dr^2}+\frac{1}{r}\frac{d}{dr}-\frac{4}{r^2}\right)\left[-H(r)+2F(r)H(r)+\left(\frac{d^2}{dr^2}+\frac{1}{r}\frac{d}{dr}-\frac{4}{r^2}\right)H(r)\right]=\frac{1}{2}\left[\frac{d^2}{dr^2}\hat{F}(r)-\frac{1}{r}\frac{d}{dr}\hat{F}(r)\right], \tag{19}$$

The Bessel operator in Eq. (19) gives that $H(r)\propto 1/r^2$ for $r\to\infty$ (see [7] for the details).

It can be shown that for any other of the higher-order perturbation functions u_n, the lowest asymptotic power is r^{-2}. This means that the full solution obeys the same asymptotic law, which can be used to specify the boundary conditions on a truncated (finite-size) computational box as follows

$$p\simeq\frac{C_p}{r^2},\quad u\simeq\frac{C_u}{r^2},\quad \text{for}\quad r=R\gg 1, \tag{20}$$

where C_p and C_u are some constants.

The main goal of the present paper is to find the proper implementation of the far-field condition Eq. (20). To this end we differentiate the functions (say function p) and acknowledge Eq. (20), namely

$$\frac{\partial p}{\partial x}\simeq-2\frac{C_p}{r^3}\frac{\partial r}{\partial x}=-C_p\frac{2x}{r^4}=\frac{2x}{r^2}p,\quad \frac{\partial p}{\partial y}\simeq-2\frac{C_p}{r^3}\frac{\partial r}{\partial y}=-C_p\frac{2y}{r^4}=-\frac{2y}{r^2}p. \tag{21}$$

On the first sight, these are two conditions on the derivatives of the sought function, and satisfying both of them would make the problem overdetermined. Actually, the two of them are interconnected, because the partial derivatives of the same function are involved. After straightforward algebra, one gets a single condition that can replace the asymptotic boundary condition on a truncated region, namely

$$x\frac{\partial p}{\partial x}+y\frac{\partial p}{\partial y}\approx-2\frac{x^2+y^2}{r^2}p=-2p,\quad r\gg 1, \tag{22}$$

which gives the following nonlocal boundary conditions at the boundaries of a finite computational box:

$$\left(x\frac{\partial p}{\partial x}+y\frac{\partial p}{\partial y}\right)|_{x=\pm L_1}=-2p(\pm L_1,y),\qquad \left(x\frac{\partial p}{\partial x}+y\frac{\partial p}{\partial y}\right)|_{y=\pm L_2}=-2p(x,\pm L_2). \tag{23}$$

The set $(x, y)\in[-L_1, L_1]\times[-L_2, L_2]$ gives the computational box. The boundary conditions for function u are the same as for p, since the asymptotic decay of the latter is the same.

Note that if the expected behavior at infinity is algebraic of n-th order ($p\simeq C_p/r^n$), then the asymptotic boundary condition are given by the following generalization of Eq. (22)

$$x\frac{\partial p}{\partial x}+y\frac{\partial p}{\partial y}\approx -np,\quad r\gg 1. \tag{24}$$

The above derived condition has a similar meaning as the so-called Perfectly Matched Layer (PML) in the numerical solutions of boundary value problems in unbounded domains that arise in electromagnetic theory (see the original work [3,20] and the monograph [19]).

5. Difference scheme

As already mentioned, the first difficulty on the way of the numerical solution of the problem under consideration is the infinite region in which the solution is sought. Clearly, there is an inevitable trade-off between the desire to make the computational box as large as possible, on the one hand, and to keep the computational resources within reasonable limits—on the other. The latter limits the size of the computational box (seed [6]), and precludes the possibility to identify numerically the precise asymptotic decay of the solution at infinity.

The important facet of a localized solution is that in the 'outer' region, the solution decays to zero, and the derivatives of different orders also vanish. This means that on a uniform grid, the truncation error also diminishes with the increase of the spatial variables. This means that a non-uniform grid can be implemented in which the spacing increases commensurate with the decrease of the sought function. The above discussed algebraic decay of the profile gives a reasonable estimate of the rate of decay needed to design the law for the non-uniform grid. After some experimentation, we have found that the optimal grid is the one in which the distance between the grid points increases exponentially with the increase of the distance form the origin of the coordinate system. Due to the obvious symmetry of the problem, we can look for the solution only in the first quadrant: $x, y\in[0, L_1]\times[0, L_2]$. We select the following rules for the non-uniform grids in the x- and y-directions:

$$x_i=\sinh[\hat{h}_1 i],\quad i=0,\ldots,N_x+1, \tag{25}$$

$$y_j=\sinh[\hat{h}_2 j],\quad j=0,\ldots,N_y+1, \tag{26}$$

where $\hat{h}_1=D_1/N_x$ and $\hat{h}_2=D_2/N_y$ and $D_{1,2}$ are selected in a manner to have large enough computational region. For instance, the choice $D_1=D_2=4.6$ provides a box [0,50] × [0,50], because $L_i=\sinh(D_i)=\sinh(4.6)\approx 49.74$. The numbers D_i can be used to make the scheme more efficient. In order to implement the nonlocal boundary conditions, the grid overlaps the region by one line at each boundary.

Now, for the above introduced variable spacings we have

$$h_i^x=x_{i+1}-x_i,\quad h_j^y=y_{j+1}-y_j. \tag{27}$$

The various difference approximations on the non-uniform grid are given by [23]:

$$\Lambda^{xx}\phi_{ij}=\frac{2\phi_{i-1j}}{h_{i-1}^x(h_i^x+h_{i-1}^x)}-\frac{2\phi_{ij}}{h_i^x h_{i-1}^x}+\frac{2\phi_{i+1j}}{h_i^x(h_i^x+h_{i-1}^x)}=\frac{\partial^2\phi}{\partial x^2}|_{ij}+O(|h_i^x-h_{i-1}^x|), \tag{28a}$$

$$\Lambda^{yy}\phi_{ij}=\frac{2\phi_{ij-1}}{h_{j-1}^y(h_j^y+h_{j-1}^y)}-\frac{2\phi_{ij}}{h_i^y h_{i-1}^y}+\frac{2\phi_{ij+1}}{h_j^y(h_j^y+h_{j-1}^y)}=\frac{\partial^2\phi}{\partial y^2}|_{ij}+O(|h_i^y-h_{i-1}^y|), \tag{28b}$$

$$\Lambda^{xy}\phi_{ij}=\frac{\phi_{i+1j+1}-\phi_{i-1j+1}-\phi_{i+1j-1}+\phi_{i-1j-1}}{(h_i^x+h_{i-1}^x)(h_j^y-h_{j-1}^y)}=\frac{\partial^2\phi}{\partial x\partial y}+O(h^x h^y). \tag{28c}$$

For a smooth distribution of the non-uniform grid for which $(\partial h^x/\partial x) \sim O(h_{i-1})$, one has

$$O(|h_i^x - h_{i-1}^x|) \approx |\frac{\partial h^x}{\partial x} h_{i-1} + \frac{1}{2}\frac{\partial^2 h^x}{\partial x^2} h_{i-1}^2| = O(|h_{i-1}|^2). \tag{29}$$

There exists a number of different ways to create an iterative algorithm. Since, the main purpose of the present work is to investigate the performance of the proposed new boundary conditions Eq. (22), we chose the so-called method of 'false transients' (see, e.g., [17]) as one of the most straightforward approaches to constructing an effective iterative procedure. The method consist of adding first derivatives with respect to an artificial time in the elliptic system rendering the latter into a parabolic one. We use the following time-stepping procedure:

$$\frac{p_{ij}^{n+1} - p_{ij}^n}{\tau} = (\lambda^{xx} + \Lambda^{yy}) p_{ij}^n - c^2 \Lambda^{yy} u_{ij}^n, \tag{30a}$$

$$\frac{u_{ij}^{n+1} - u_{ij}^n}{\tau} = \beta_2(\lambda^{xx} + \Lambda^{yy}) u_{ij} - \theta^n (u_{ij}^n)^2 + p_{ij}^{n+1} - u_{ij}^n - \beta_1 c^2 \Lambda^{yy} u_{ij}^n, \tag{30b}$$

for $i = 0, \cdots, N_x$, $j = 0, \cdots, N_y$ except the point $i = 0$, $j = 0$. Then we have a parameter: the time increment τ, which can be used to manipulate the speed of convergence.

Now, the reasons to replace the original fourth order elliptic equation by a system of two second-order equations become transparent. The first is that one can introduce an artificial time rendering the problem to a parabolic one, and the second is the representing as a system reduces the condition number for each of the matrices involved, making the iterations converge significantly faster.

The system is coupled by the symmetry conditions, the approximation of the bifurcation condition, and the boundary conditions. The symmetry conditions are acknowledged by the special approximation of the main operators at the lines of symmetry $i = 0$ and $j = 0$:

$$\Lambda^{xx}\phi_{0j} = \frac{2\phi_{1j} - 2\phi_{0j}}{(h_0^x)^2}, \quad \Lambda^{yy}\phi_{i0} = \frac{2\phi_{i1} - 2\phi_{i0}}{(h_0^y)^2}, \quad \Lambda^{xy}\phi_{0j} = \Lambda^{xy}\phi_{i0} = 0. \tag{31}$$

Basing on the above approximation, one can approximate the bifurcation condition as follows

$$\tilde{\theta} = \frac{-\beta_2(\Lambda^{xx}u_{00}^n + \Lambda^{yy}u_{00}^n) + u_{00}^n + \beta_1 c^2 \Lambda^{yy} u_{00}^n - p_{00}^n)}{u_{00}^n}, \quad \theta^{n+1} = (1-\tau)\theta^n + \tilde{\theta}. \tag{32}$$

Introducing the relaxation in the last equation makes the iterations stable for larger τ.

The key element of the present work is the approximation of the nonlocal asymptotic boundary conditions Eq. (23). By the virtue of the selected geometry of the grid, the so-called 'numerical infinities' are given by $i = N_x$ and $j = N_y$. We chose the following approximation of Eq. (23) at the numerical infinities:

$$p_{iN_y+1}^{n+1} = p_{iN_y-1}^{n+1} + \frac{h_{N_y}^y + h_{N_y-1}^y}{y_{N_y}} \left[-2p_{iN_y}^{n+1} - \frac{x_i}{h_i^x + h_{i-1}^x}(p_{i+1N_y}^{n+1} - p_{i-1N_y}^{n+1}) \right], \quad i = 0, \ldots, N_x, \tag{33a}$$

$$p_{N_x+1j}^{n+1} = p_{N_x-1j}^{n+1} + \frac{h_{N_x}^x + h_{N_x-1}^x}{x_{N_x}} \left[-2p_{N_xj}^{n+1} - \frac{y_j}{h_j^y + h_{j-1}^y}(p_{N_x+1j}^{n+1} - p_{N_x-1j}^{n+1}) \right], \quad j = 0, \ldots, N_y. \tag{33b}$$

The above approximations are implicit, but they do not require solving algebraic systems at the boundary grid lines, because the conditions Eqs. (33) are actually used to compute the new values (time stage $(n+1)$) of the unknown functions on the lines that overlap the main grid. Thus, after the $n+1$-st iteration is computed on all grid points (including the boundary points) from Eq. (30), the values on the overlapping grid lines are explicitly computed from Eqs. (33).

6. Validations of the algorithm

The first test is to show that the approximation is consistent on different grids. We computed the solution for four different grid sizes ranging from 20 intervals to 160 intervals in each direction. For this test we chose $c = 0.5$ and $D_1 = D_2 = 4.6$ In Fig. 1 we show the result for the two main cross-sections of the profile for four different grid

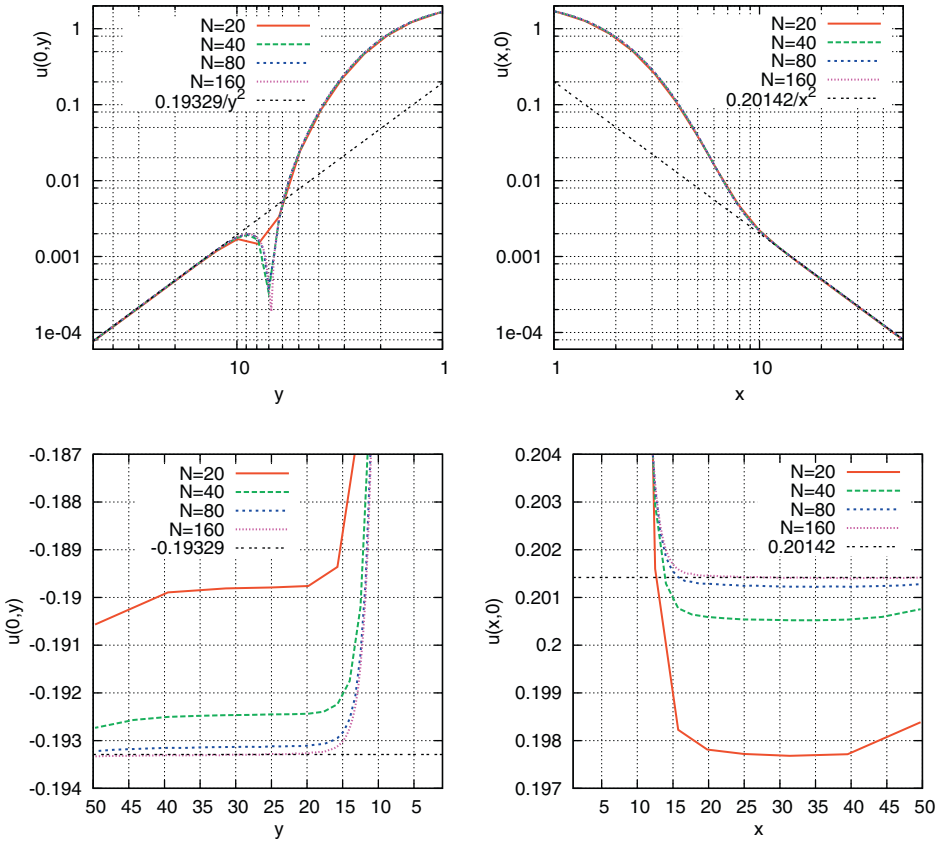

Fig. 1. The effect of the grid size for $\beta_1 = 1$, $c = 0.2$. Upper panels: the function. Lower panels: the function scaled by r^2.

sizes, $N = N = N_x = N_y$. Here and henceforth we present the results in log–log plots, because we need to examine the performance of the numerical scheme for very far distances from the center and to verify that the asymptotic decay of the solution is well captured by the new implementation of the boundary conditions. One can see that the profile exhibits a quadratic algebraic decay at infinity which is uniform up to the last grid point at the boundary. The upper panels show the shape function in the respective cross-section, while the lower panels present the same function scaled by the expected asymptotic behavior. One can see that for large distance from the origin of the coordinate system the scaled profile approaches a constant. Naturally, this constant depends on the grid size, and the observed dependence splendidly confirms the second order of approximation of the scheme if the three finer resolutions are considered.

The next important validation of the numerical technology developed here is to understand the role of the size of computational box. As already mentioned, if the trivial Dirichlet conditions are imposed at infinity, the influence of the finite size is quite considerable, and one needs to have very large computational box. The results of this test are presented in Fig. 2. The upper panels present linear plots in the region of the significant amplitude of the profile. The lower panels show the log–log plots in the far-out region. The results show that differences are insignificant even next to the computational boundary. The size $L \approx 333$ gives good results even for the case $c = 0.9$ when the profile is much larger at infinity.

7. Results for the soliton shapes

We have applied the algorithm developed here, and performed a detailed parametric study of the shapes of the 2D stationary propagating localized waves of the PBE.

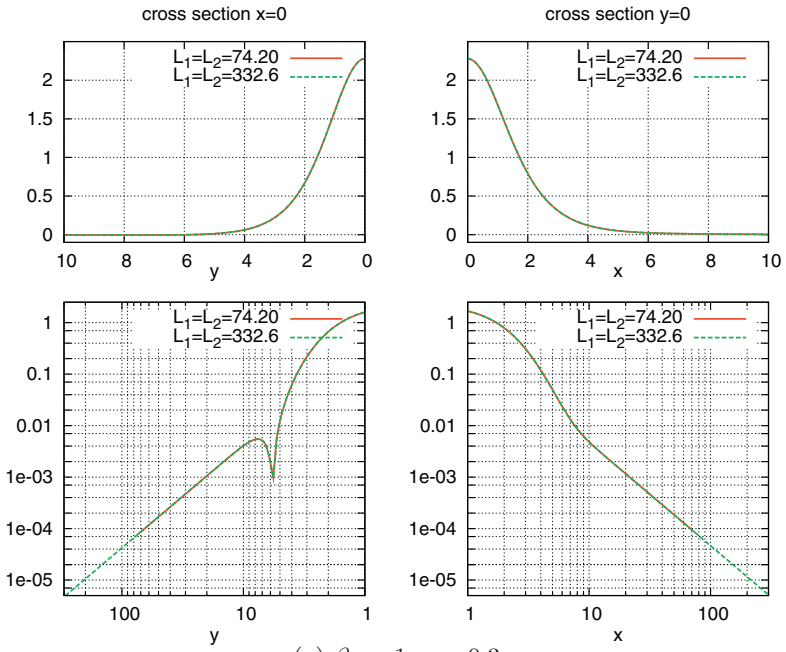

(a) $\beta_1 = 1$, $c = 0.3$

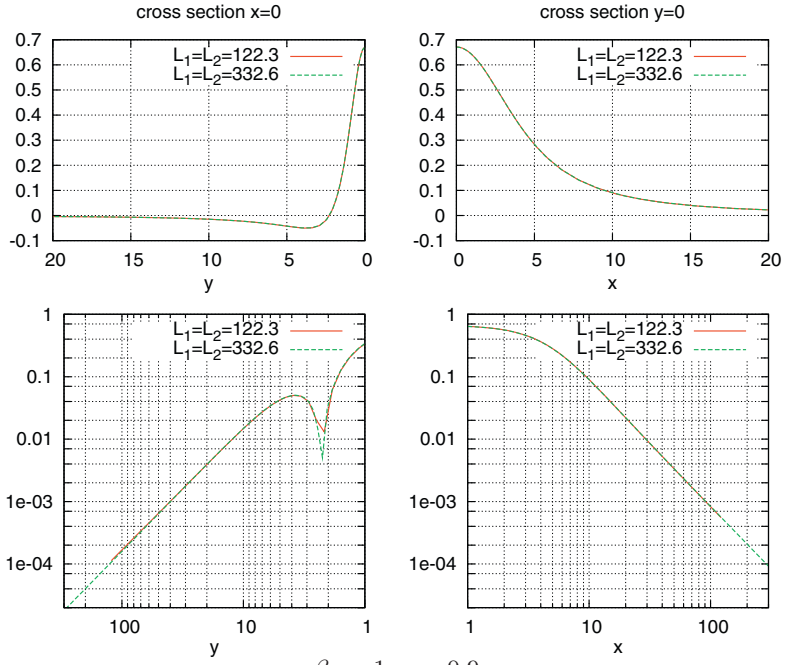

$\beta_1 = 1$, $c = 0.9$

Fig. 2. The role of the size of computational box.

7.1. *Effect of the phase speed c*

First we fix $\beta_1 = 1$ and investigate the effect of the magnitude of the phase speed on the shape of the soliton. In Fig. 3 we present the two main cross-sections of the profiles. In the left panels is depicted the profile in the longitudinal cross-section $x = 0$, while in the right panels is the lateral cross-section $y = 0$. The upper row of panels present linear plots, while the lower row of panels are log-log plots. As already above mentioned, the log–log plots are essential in

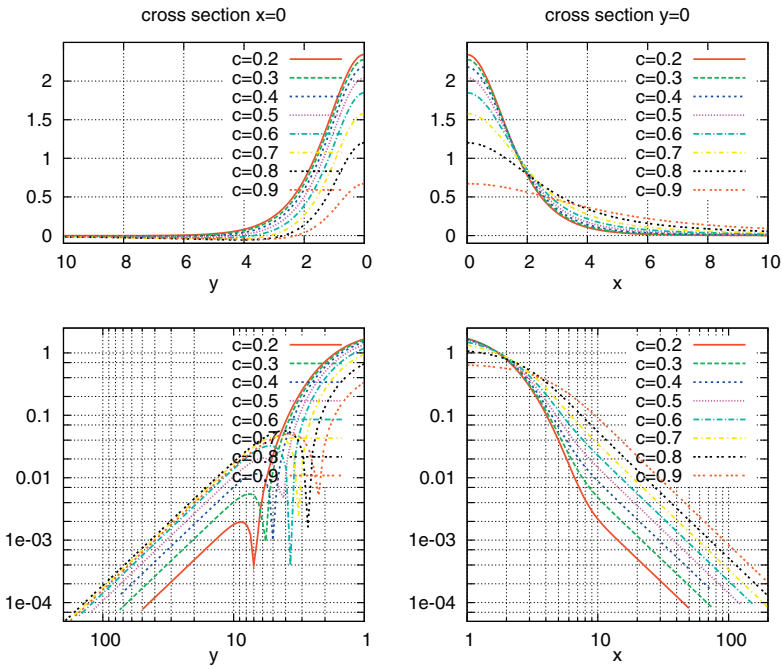

Fig. 3. Crossections for $\beta_1 = 1$ and different c.

identifying the algebraic decay of the profiles at infinity. Indeed one can see the perfect lines of slope -2 to which both the longitudinal and the lateral profiles asymptote.

It has already been above mentioned that depressions form in the front and the back of the wave. These depressions are not very deep, and can be reliably identified only on the log–log plots. In the latter, the absolute value of the profile is plotted, and the point where the sign of the profile changes (the 'edge of the depression') there is a marked 'dip' in the shape. An important observation that can be made from Fig. 3 is that the height of the soliton decreases with the increase of the phase speed c, while the length of the support increases. This in agreement with the similar behavior of the subcritical 1D solitons [11,13,15]. The existence of depressions in 2D was first reported in [6] for the BE, where a standard difference scheme on uniform grid with simple Dirichlet boundary conditions was used for the numerical solution. This novel and not entirely intuitive feature was confirmed independently by a spectral technique in [8]. In the case of the unsophisticated difference scheme [6], there could have been some slight doubts about the reality of this effect, because of the possible deformation of the profile due to the insufficient size of the computational box. The spectral scheme is free of this shortcoming, and so is the approximation given in the present paper. Here both limitations are removed: the computational box is now very large, and the boundary condition is a 'milder' condition of behavioral type (see [5] for definition) or, alternatively, of PML-type [3,19,20]. The present results can be considered as a demonstration of the excellent performance of the proposed numerical approach at the one hand, and as a confirmation of this critical new phenomenology of the 2D solutions of the Boussinsq equations—on the other. In this instance the effect is similar to the one reported for the solutions of the KP equation localized in one of the directions [21,22].

In Fig. 4 we present the 2D shapes for different phase speeds c and fixed value of the dispersion coefficient $\beta_1 = 1$. One can see that for small and moderate c, the depressions are virtually undetectable on the graph, while for large c they become very well pronounced. An important comment is due here about the apparent relative contraction of the profile in the direction of propagation. Judging by the edge of the depression, one might be tempted to conclude that there is some kind of relative contraction in the direction simultaneously with the increase of the support in the lateral direction. We did attempt to argue the relative contraction in [6,8], but such a conclusion is not precise. The fact is that the support has to be defined as the edge of the absolute value of the profile where the latter becomes smaller than certain value, say 0.01. In the light of this comment, the length of the support has to be defined as the radius of the circle that encompasses the depressions shown in the right panel of Fig. 4.

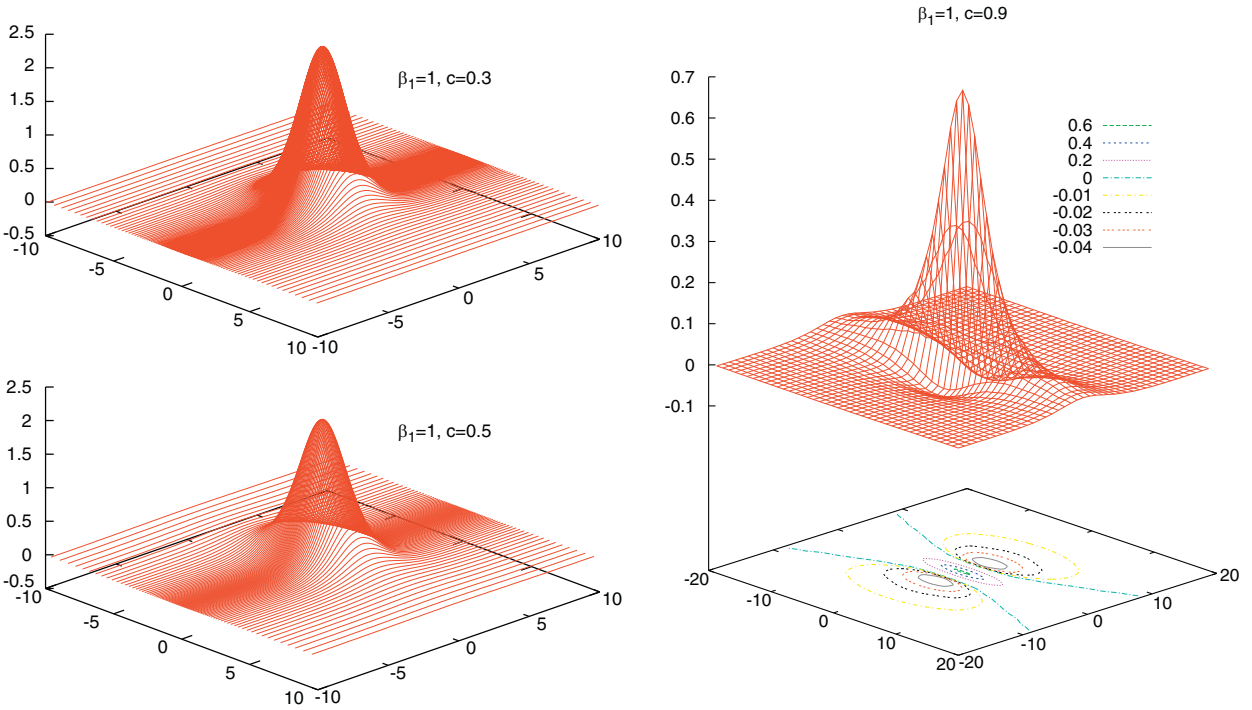

Fig. 4. 2D profiles for $\beta_1 = 1$ and different c.

7.2. *Role of the dispersion parameter β_1*

The next series of numerical experiments are aimed at elucidating the effect of the magnitude of the dispersion parameter β_1 on the profile shape. The result in terms of the two main cross-sections is presented in Fig. 5 for fixed

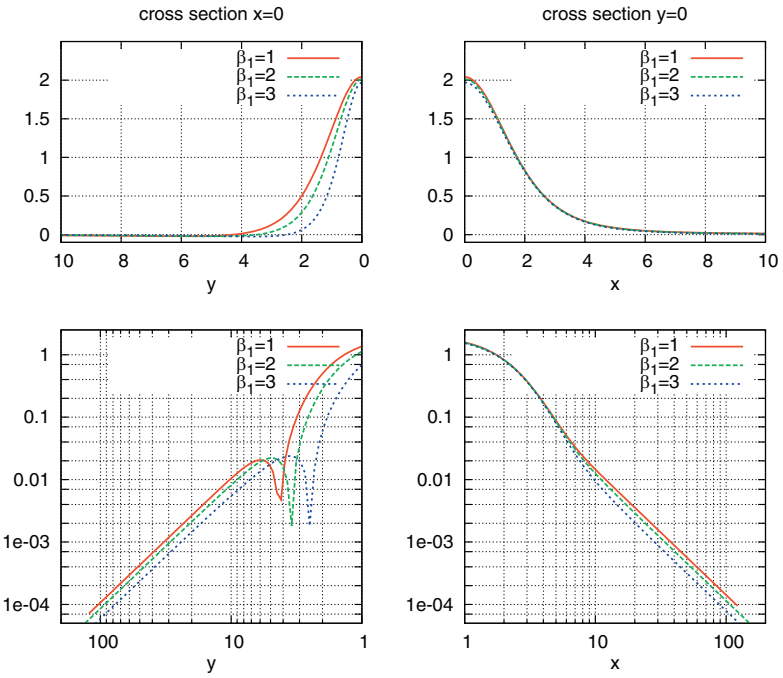

Fig. 5. Crossections for $c = 0.5$ and different β_1.

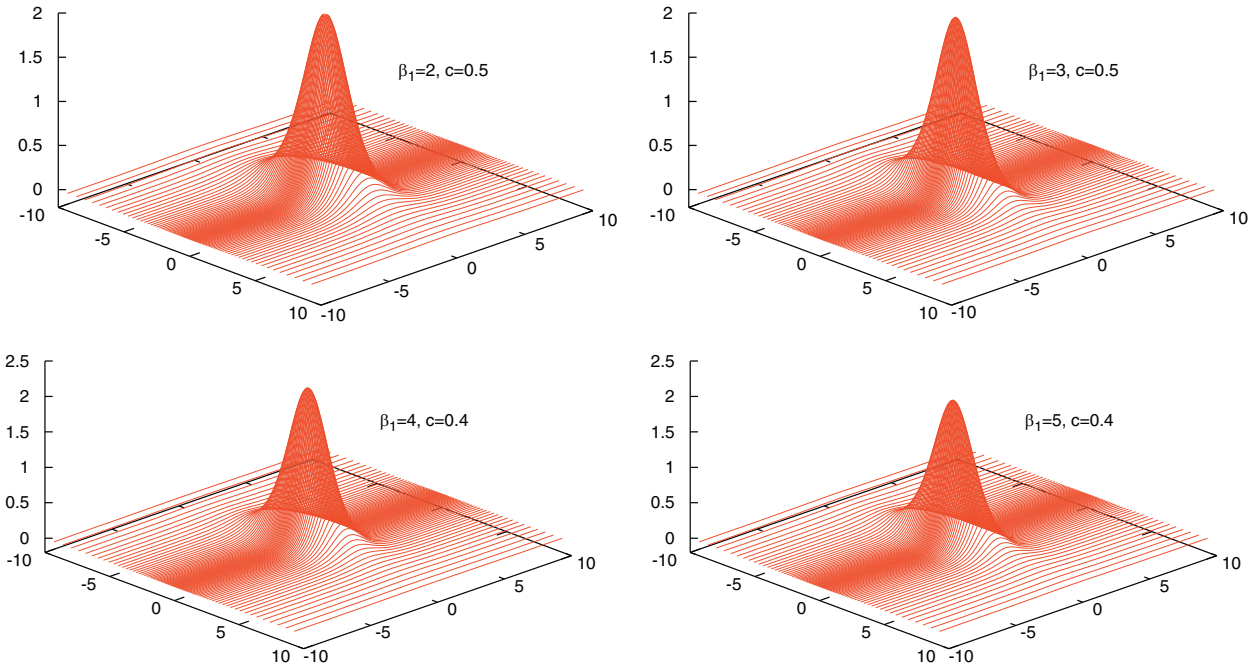

Fig. 6. 2D profiles for different β_1.

$c = 0.5$ and three different $\beta_1 = 1,2,3$. Comparing the results from Fig. 5 to Fig. 3 allows one to conclude that the increase of β_1 for a given c has the same effect as the increase of c for a given β_1: it leads to contracting the positive part of the shape and to deepening the forerunning and trailing depressions. The 2D shapes for the two of the cases presented in Fig. 5 are given in the upper panels of Fig. 6. The lower panels of this figure give the result for even larger $\beta_1 = 4$ and $\beta_1 = 5$, respectively. Note that results for these β_1s could not be obtained with $c = 0.5$. There is a limit in c for which the shapes exist numerically for given β_1, which phenomenon is elucidated in the next subsection.

7.3. Limitations for the existence of stationary propagating 2D wave

The 1D *sech*-soliton of BPE, Eq. (3), has some specific features that are not known for the cases of BE and RLWE. First of all, there is a case, namely $\beta_1 = \beta_2$, when the solution exist for all c. Note that the *sech* solitons of BE are strictly subcritical ($c < 1$), while those for RLWE are supercritical ($c > 1$). For $\beta_1 \neq \beta_2$; there exist both subcritical solitons in the interval $|c| \in [0, \min\{1, \sqrt{\beta_2/\beta_1}\}]$, and supercritical ones in the interval $|c| \in [\max\{1, \sqrt{\beta_2/\beta_1}\}, \infty]$. In the subcritical branch, if c increases, the amplitude and support ('effective width') decrease. Alternatively, in the supercritical branch, if c increases, the amplitude increases but the support decreases (the peak is sharper).

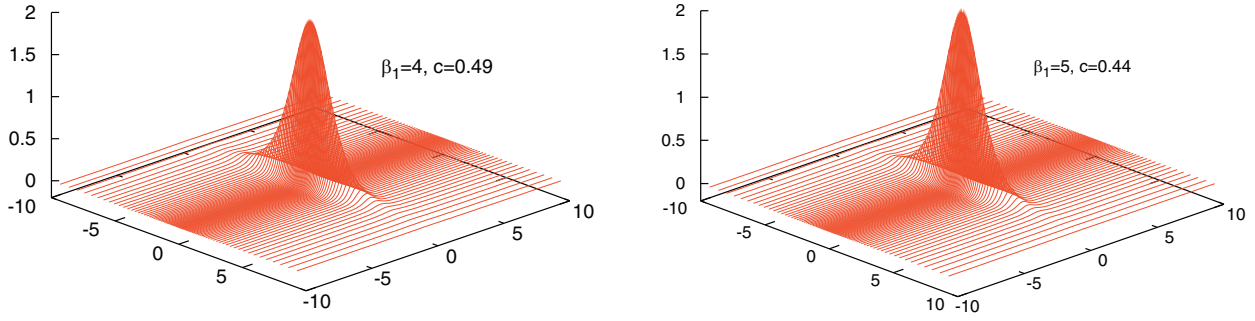

Fig. 7. The solitons shapes ner the threshold of non-existence.

Table 1
Comparison between the analytical limit of solutions in 1D with maximal c reached numerically in 2D ($\beta_2 = 1$).

β_1	1	2	3	4	5
$\sqrt{\beta_2/\beta_1}$	1.000	0.707	0.577	0.500	0.447
max c	0.99	0.7	0.55	0.49	0.44

The situation is rather different in 2D: for supercritical phase speeds the governing Eq. (5) is no longer elliptic in space. This means that localized structure of the sought type does not exist. For this reason, we focus in the present work on the subcritical solutions of the 2D BPE. We have presented the results for β_1 when c that are close enough to the border of existence of the 1D soliton. For each value of β_1 we have increased c until we failed to get a solution. Fig. 7 gives an example of our findings for $\beta_1 = 4$ (left panel) and $\beta_1 = 5$ (right panel) for which the respective 'terminal' values for the phase speed are $c = 0.49$ and $c = 0.44$. Once again, one can see that for phase speed close to the threshold of non-existence, the cross-section that corresponds to the edge of the depression becomes an ellipse of very small axis in the direction of propagation. Table 1 shows that the limit of non-existence of the 2D solitons virtually coincides with the analytical result for the 1D solitons. Thus, we are unable to reach convergence for 2D solitons with phase speeds faster than the respective limiting phase speeds of the 1D solitons.

8. Conclusions

The Boussinesq Paradigm Equation (BPE) for waves on the surface of shallow inviscid layer is considered and its solitary-wave solutions are investigated numerically. The shape of stationary propagating solitary wave is a solution of a fourth-order nonlinear elliptic equation in an infinite domain. The bifurcation nature of the problem is addressed by a special algorithm involving scaling of the dependent variable. A new nonlocal approximation of the asymptotic boundary conditions at the finite boundaries of the computational box is proposed. Relatively sparse non-uniform grids are used in both spatial directions that allow computations in large computational domains. An iterative difference scheme is devised using false-transients and the stationary solutions are obtained after the iterations converge. The second order approximation of the scheme is verified via computations on grids of different sizes.

The shape of the steadily propagating 2D localized solution of BPE is obtained for different values of the governing parameters: phase speed, and two dispersion parameters. The algebraic asymptotic decay is confirmed with high accuracy. A pseudo-Lorentzian elongation of the support of the solitary wave is uncovered. In the longitudinal direction depressions are formed in the front and in the rear of the wave are. They make the wave appear shortened in the direction of the motion. The obtained here profiles can be used as initial conditions in time dependent computations for verifying if they are robust structures, and eventually, for the interaction of 2D solitons of this type.

Acknowledgement

This research has been supported in part by a grant from Louisiana Board of Regents through contract NSF(2009)-PFUND-156.

References

[1] M.J. Ablowitz, H. Sigur, Solitons and the Inverse Scattering Transform, SIAM, Philadelphia, 1981.
[2] T.B. Benjamin, J.L. Bona, J.J. Mahony, Model equation for long waves in nonlinear dispersive systems, Phil. Trans. R. Soc. Lond. A272 (1972) 47–78.
[3] J.-P. Berenger, A perfectly matched layer for the absorption of electromagnetic waves, J. Comp. Phys. 114 (1994) 185–2000.
[4] J.V. Boussinesq, Théorie des ondes et des remous qui se propagent le long d'un canal rectangulaire horizontal, en communiquant au liquide contenu dans ce canal des vitesses sensiblement pareilles de la surface au fond, J. Math. Pure Appl. 17 (1872) 55–108.
[5] J.P Boyd, Chebishev Fourier Spectral Methods, second ed., Dover, New York, 2001.
[6] J. Choudhury, C.I. Christov, 2D solitary waves of Boussinesq equation, in: ISIS International Symposium on Interdisciplinary Science, Natchitoches, October 6–8, 2004, APS Conference Proceedings 755, Washington, DC, 2005, pp. 85–90.
[7] J. Choudhury, C.I. Christov, Stationary-Propagating Solutions of the Boussinesq Equation In 2D, VDM Verlag, 2009.
[8] M.A. Christou, C.I. Christov, Fourier–Galerkin method for 2D solitons of Boussinesq equation, Math. Comput. Simul. 74 (2007) 82–92.
[9] M.A. Christou, C.I. Christov, Galerkin spectral method for the 2d solitary waves of boussinesq paradigm equation, in: AIP Conf. Proc, vol. 1186, 2009.

[10] C.I. Christov, A complete orthonormal sequence of functions in $L^2(-\infty\ \infty)$ space, SIAM J. Appl. Math. 42 (1982) 1337–1344.
[11] C.I. Christov, Conservative difference scheme for Boussinesq model of surface waves, in: W.K. Morton, M.J. Baines (Eds.), Proc. ICFD V, Oxford University Press, 1995, pp. 343–349.
[12] C.I. Christov, Fourier–Galerkin algorithm for 2D localized solutions, Annuaire de l'Univ. Sofia, Livre 2 - Mathématiques Appliqee et Informatique 89 (1995) 169–179.
[13] C.I. Christov, An energy-consistent Galilean-invariant dispersive shallow-water model, Wave Motion 34 (2001) 161–174.
[14] C.I. Christov, G.A. Maugin, A. Porubov, On boussinesq's paradigm in nonlinear wave propagation, C. R. Mecanique 335 (2007) 521–535.
[15] C.I. Christov, M.G. Velarde, Inelastic interaction of Boussinesq solitons, J. Bifurcat. Chaos 4 (1994) 1095–1112.
[16] I. Christov, C.I. Christov, P.M. Jordan, Modeling weakly nonlinear acoustic wave propagation, Q. J. Mech. Appl. Math. 60 (4) (2007) 473–495.
[17] G.D. Mallison, G. de Vahl Davis, The method of false transients for the solution of coupled elliptic equations, J. Comput. Phys. 12 (1973) 435–461.
[18] A.C. Newell, Solitons in Mathematics and Physics, SIAM, Philadelphia, 1985.
[19] A.C. Polycarpou, Introduction to the Finite Element Method in Electromagnetics, Morgan & Claypool, 2006.
[20] A.C. Polycarpou, M.R. Lyons, C.A. Balanis, A two-dimensional finite element formulation of the perfectly matched layer, IEEE Microw. Guided Wave Lett. 6 (1996) 338–340.
[21] A.V. Porubov, G.A. Maugin, V.V. Mateev, Localization of two-dimenasional non-linear strain waves in a plate, Nonlinear Mech. 39 (2004) 1359–1370.
[22] A.V. Porubov, F. Pastrone, G.A. Maugin, Selection of two-dimensional nonlinear strain waves in micro-structured media, C. R. Mecanique 332 (2004) 513–518.
[23] A.A. Samarskii, E. Nikolaev, Numerical Methods for Grid Equations volume 1, Birkhauser, Basel, 1989.
[24] N.J. Zabusky, M.D. Kruskal, Interaction of 'solitons' in collisionless plasma and the recurrence of initial states, Phys. Rev. Lett. 15 (1965) 240–243.